



# 1 Measurement of spatio-temporal changes of cave ice using geodetic 2 and geophysical methods: Dobšiná Ice Cave, Slovakia

3  
4  
5 Katarína Pukanská<sup>1</sup>, Karol Bartoš<sup>1</sup>, Juraj Gašinec<sup>1</sup>, Roman Pašteka<sup>2</sup>, Pavol Zahorec<sup>3</sup>, Juraj Papčo<sup>4</sup>,  
6 Ľubomír Kseňák<sup>1</sup>, Pavel Bella<sup>5,6</sup>, Erik Andrassy<sup>2</sup>, Laura Dušeková<sup>5</sup>, Diana Bobíková<sup>1</sup>

7 <sup>1</sup> Institute of Geodesy Cartography and GIS, Technical University of Košice, Košice, 04001, Slovakia

8 <sup>2</sup> Department of Engineering Geology, Hydrogeology & Applied Geophysics, Comenius University in Bratislava, Bratislava,  
9 814 99, Slovakia

10 <sup>3</sup> Earth Science Institute, Slovak Academy of Sciences, Banská Bystrica, 97401, Slovakia

11 <sup>4</sup> Department of Theoretical Geodesy and Geoinformatics, Slovak University of Technology in Bratislava, Bratislava, Slovakia

12 <sup>5</sup> Slovak Caves Administration, Liptovský Mikuláš, 031 01, Slovakia

13 <sup>6</sup> Department of Geography, Faculty of Education, Catholic University in Ružomberok, Ružomberok, 0340 01, Slovakia

14  
15  
16 *Correspondence to:* K. Bartoš (karol.bartos@tuke.sk)

17 **Abstract:** Dobšiná Ice Cave has attracted the attention of many researchers since its discovery more than 150 years ago.  
18 Although the cave is located outside the high-mountain area, it hosts one of the largest blocks of underground perennial ice.  
19 The topographic mapping of this unique UNESCO Natural Heritage site has led to several historical surveys. In the last decades  
20 of rapid climate change, this natural formation has been subject to rapid changes that are dynamically affecting the shape of  
21 the ice body. Not only increased precipitation, the rise in year-round surface temperatures, but also the gravity cause significant  
22 shape changes in the ice filling. This paper describes modern technological tools to comprehensively survey and evaluate  
23 interannual changes in both the floor and wall of the underground ice block. Technologies such as digital photogrammetry, in  
24 conjunction with precise digital tacheometry, make it possible to detect ice accumulation and loss, including the effect of  
25 sublimation due to airflow, as well as sliding movements of the ice block to the lower part of the cave. In the last two years,  
26 geophysical methods (microgravimetry and ground penetrating radar) have been added to determine the thickness of the floor  
27 ice in the upper parts of the cave due to the complexity of the measurements. The paper not only highlights the current  
28 technological possibilities but also points out the limitations of these technologies and then sets out solutions with a proposal  
29 of technological procedures for obtaining accurate geodetic and geophysical data.

30  
31 **Key words:** Ice cave, cryomorphological topography, tacheometry, photogrammetry, laser scanning, SLAM,  
32 microgravimetry, ground penetrating radar.  
33  
34



35

## 36 **1 Introduction**

37 The dynamics of the evolution of the ice filling of caves is a long-standing scientific problem. The world of fragile underground  
38 ice caves offers its beauty in many countries around the world. Their uniqueness attracts the attention of many researchers as  
39 well as the general public (Perşoiu and Lauritzen, 2018). Since the first discoveries of these unique natural beauties, researchers  
40 have noticed that the ice fill is subject to change over time. Their research focuses primarily on the morphology and the  
41 dynamics of the glacier's shape changes depending on the climatic conditions prevailing underground, but also on their age  
42 dating, genesis, and geographic location. Awareness of the world's ice caves was relatively small until the 19<sup>th</sup> century and  
43 narrowly geographically confined to Central Europe and Russia. Ice caves in Jura and the Western Alps (now France and  
44 Switzerland) have been known for a long time, but Dobšiná Ice Cave, together with Demänovská Cave (Slovakia) and Pestera  
45 Scărisoara Cave (Romania), are among the first caves discovered in the 19<sup>th</sup> century in Central Europe outside the Alpine  
46 regions (Meyer, 2018). As stated by Meyer (2018), the history of ice cave exploration in the more distant past (19<sup>th</sup>-20<sup>th</sup>  
47 century) was devoted to the unification of heterogeneous nomenclature, to the description of phenomena influencing the  
48 formation of ice in caves - depending on the airflow pattern, climatic conditions (defining the relationship between internal  
49 and external climatic conditions, microclimate, climate in front of the cave, as well as regional macroclimate), cave shapes.  
50 Many of these theories have been contradicted and disproved over time.

51 In the past, ice level was typically measured as the distance from a fixed point (monitoring datum) on the cave wall or ceiling  
52 above the ice floor (marked by a screw or nail permanently inserted into the rock) to the surface of the ice floor (Smith, 2014).  
53 When multiple observations from a cave were available for a given year, the data offered the opportunity to model inter-annual  
54 variation in ice height. However, modern geodetic and geophysical tools after 2010 provide quite different qualitative results  
55 for surveying ice-fill dynamics (Behm, 2008; Podsushin, 2008; Hausmann, 2011; Gómez-Lende, 2014). Digital tacheometry  
56 and, more recently, terrestrial laser scanners, or digital photogrammetry tools, allow the collection of data with high temporal  
57 and spatial resolution. These technologies have been highly proven in many research works (for instance, Pukanská et al.,  
58 2018; Šupinský et al., 2019; Pukanská et al., 2020; Bella et al., 2021). The measurements have been used to detect bulk masses  
59 or to trace some ice blocks but mainly to survey the geomorphological features of cave spaces - cartographic and topographic  
60 representation or the creation of geological maps (Petters, 2011; Berenguer-Semper, 2014; Milius, 2012).

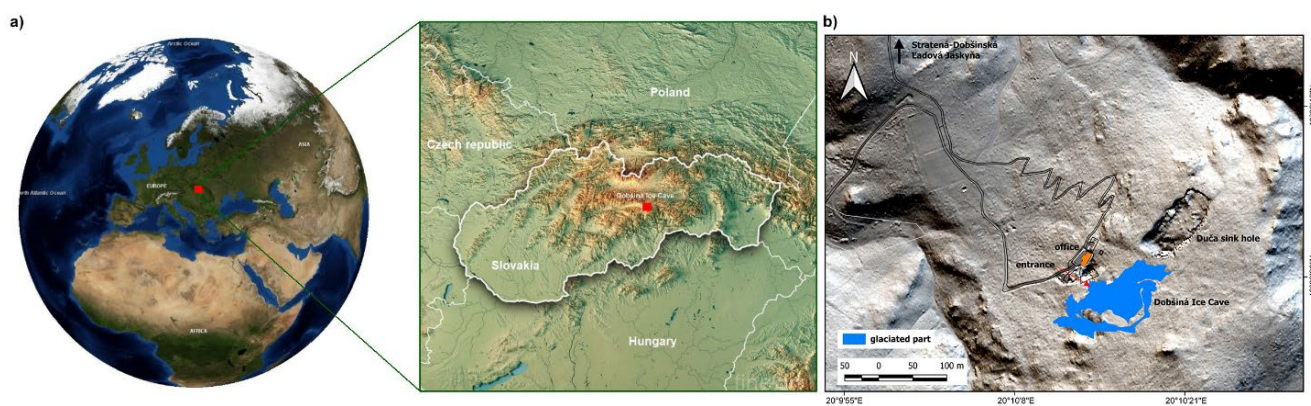
61

62 Over time, as the technology and methodologies of topographic research have evolved, so have the knowledge and refinement  
63 of scientific results. From the early historical geodetic measurements with optical instruments, and analog photogrammetry,  
64 we are now moving to technologies such as digital tacheometry and photogrammetry, terrestrial laser scanning (TLS), or  
65 modern geophysical methods such as microgravimetry, ground penetrating radar (GPR), and seismometry.



## 66 2 Study area

67 The Dobšiná Ice Cave ("Dobšinská ľadová jaskyňa" in Slovak) belongs to the well-known ice cave in the world. It is located  
68 in the southern part of Slovenský raj (Slovak Paradise) National Park in the Spiš-Gemer Karst (north of the town of Dobšiná)  
69 (Fig.1). Its entrance lies at 969 m a.s.l., on the right side of the Hnilec River valley, on the west slope of the Duča Plateau, 130  
70 m above the valley bottom. The length of the cave is 1483 m with a vertical span of 112 m. It is an inflow part of the larger  
71 genetic system of the Stratenská Cave, which is longer than 23.6 km. The whole system was formed by two underground  
72 streams - the Hnilec River and the Tiesňava Stream in the Late Pliocene (Tulis and Novotný, 1989; Novotný, 1993; Novotný  
73 and Tulis, 1996, 2005; Bella et al., 2014). The conditions for the formation of the ice fill were probably created in the Middle  
74 Pleistocene after the collapse of the ceilings (Duča sinkhole) and the breaking of the passage between Dobšinská Ice Cave and  
75 Stratenská Cave (Novotný and Tulis, 1996). At present, it is mostly filled with ice that reaches the ceiling in some places, and  
76 that divides the cavity into several parts: Small Hall, Great Hall, Collapsed Chamber, Ruffiny' Corridor, Ice tunnel, Ground  
77 Floor, and Hell. The ice filling of the cave is mainly made of floor and wall ice, ice stalagmites, and icefalls (Fig. 2). In 1995,  
78 a joint geodetic and geophysical survey of the ice volume and area was carried out, which revealed the ice volume was 110,132  
79 m<sup>3</sup>, the surface of ice fill was 9772 m<sup>2</sup>, the maximal thickness of floor ice reached 26.5 m, and the average thickness of floor  
80 ice was 13 m (Novotný and Tulis, 1996; see also Bella, 2006, 2018; Bella and Zelinka, 2018; Bella et al., 2020). The surface  
81 area (in the vicinity of the cave) is in the moderately cool (mean annual air temperature 4,7 °C; mean air temperature in January  
82 -5,4 °C, in July 14,2 °C) and very humid subregion (mean annual precipitation total 900–1000 mm) (according to Lapin et al.,  
83 2002; Faško and Šťastný, 2002; Šťastný et al., 2002).



84  
85 **Figure 1** a) Dobšiná Ice Cave, Slovakia (Ramspott, 2017); b) projection of the glaciated part of the cave on the surrounding  
86 digital terrain model (source of the DTM - LiDAR data: ÚGKK SR).



87

88 **Figure 2** Great Hall and ice tunnel (source: authors).

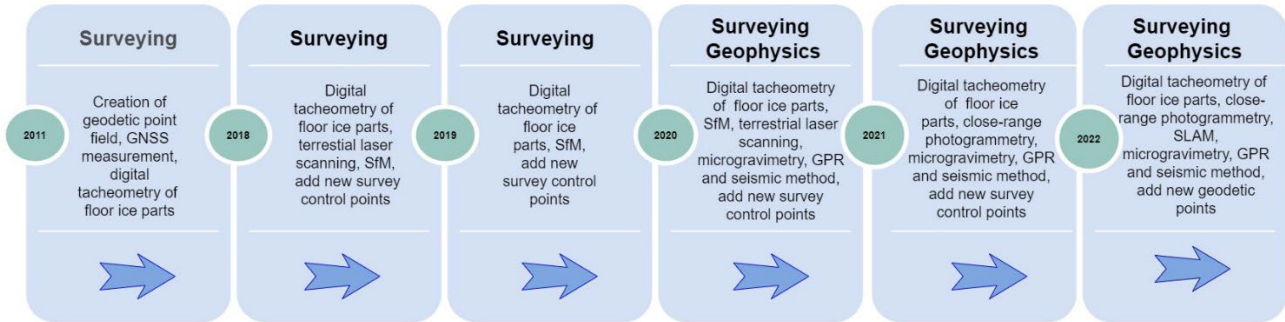
89 **3 Material and methods**

90 Although the "ice hole" under the Duča had been known to shepherds and loggers for a long time, it was discovered only on  
91 15 June 1870 by Eugene Ruffini and Co. (Lalkovič, 2000; Kudla 2020). The cave was opened to the public on 8 March 1871.  
92 The first map of the Dobšiná Ice Cave was made by its discoverer Eugen Ruffiny in 1871; later, new drawings were added.  
93 The first stereophotogrammetric surveys of the cave spaces were carried out in 1936. Another measurement was the research  
94 of spatial changes of the ice fill by geodetic and photogrammetric methods in the years 1976-1990, in which the Department  
95 of Mine Surveying and Geophysics of the Technical University of Košice (VŠT Košice) was also involved.

96 **3.2 Methodology of ice cave mapping**

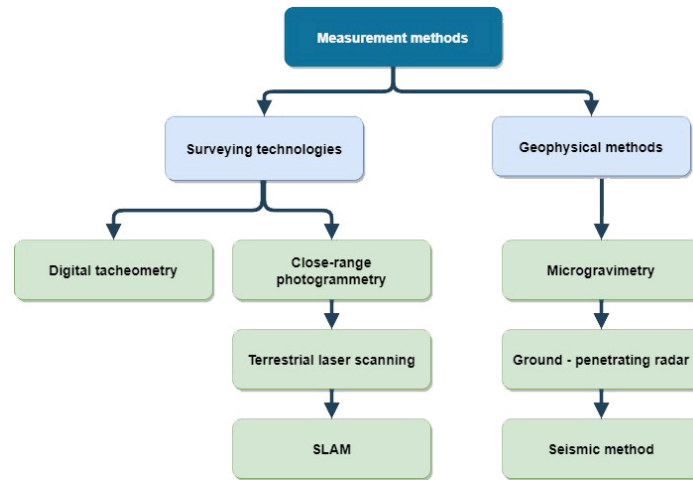
97 Dobšiná Ice Cave is a significant geomorphological and geological object of world importance. Research of changes in the ice  
98 surface due amount and composition of surface precipitation, the temperature of the internal environment, speed and direction  
99 of airflow, as well as anthropogenic factors (number of visitors, human interference), must be carried out by precise geodetic  
100 and geophysical measurements, which use detailed measurements of small surface changes and can also capture the dynamics  
101 of change over time. Geodetic methods such as digital tacheometry, but also modern non-contact technologies (digital  
102 photogrammetry and laser scanning), as well as geophysical methods such as microgravimetry and ground penetrating radar,  
103 provide an innovative way for the study of surface and volume changes of the underground ice. The systematic measurement  
104 of surface ice changes started in 2011, with the first step being the monumentation of the geodetic point field and its survey as  
105 a closed traverse, followed by its adjustment and connection to the national spatial network by GNSS measurements. Since  
106 2011, the survey methodology has been gradually complemented by newly available technologies (Figs. 3 and 4).





107  
 108 **Figure 3** The timeline of geodetic and geophysical surveys.  
 109

110 The acquisition of spatial data on the ice surface of horizontal and vertical parts of the ice-filling and the subsequent analysis  
 111 of its changes is fundamentally affected by the fact that the ice surface has a variable structure and electromagnetic radiation  
 112 can penetrate it. This has influenced the way in which the survey and the choice of appropriate technologies were made. Using  
 113 our established methodology, we propose methodological procedures that eliminate the influence of factors negatively  
 114 affecting the results of measurement and spatial model building (Fig. 4).

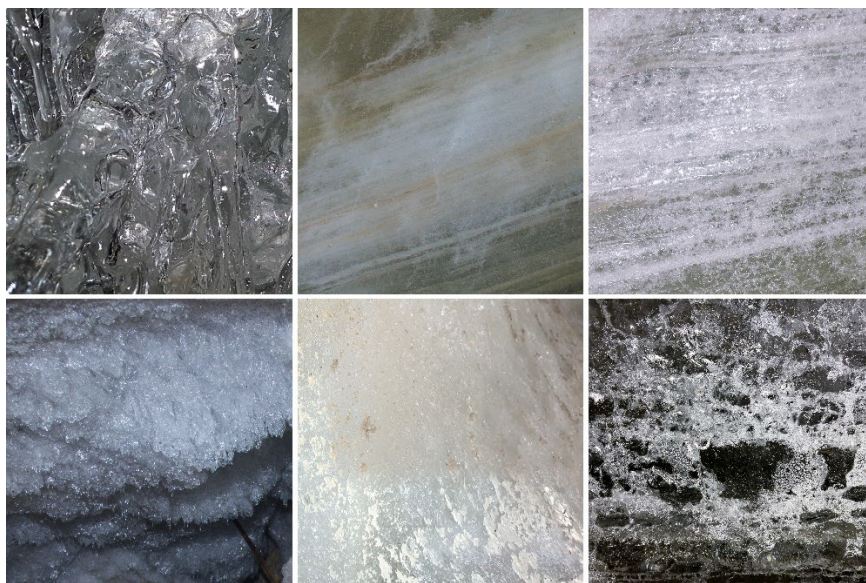


115  
 116 **Figure 4** Overview of surveying and geophysical methods.  
 117

118 When EMR passes from one environment to another, there is absorption, refraction, reflection, and transmission as the speed  
 119 of propagation of EMR changes, as well as the humidity and temperature, in the different environments. The refractive index  
 120 of water as a liquid is 1.333. In the solid state, it can be determined to be around 1.309. Materials with a higher refractive index  
 121 are more sensitive to temperature change. The interaction of electromagnetic radiation with ice and media containing ice, but  
 122 also snow, is described by the refractive index and absorption coefficient, which are functions of the wavelength. Volume  
 123 reflectivity, absorption, and transmittance are further influenced by the grain size of snow, ice, and bubbles (Warren, 2019).

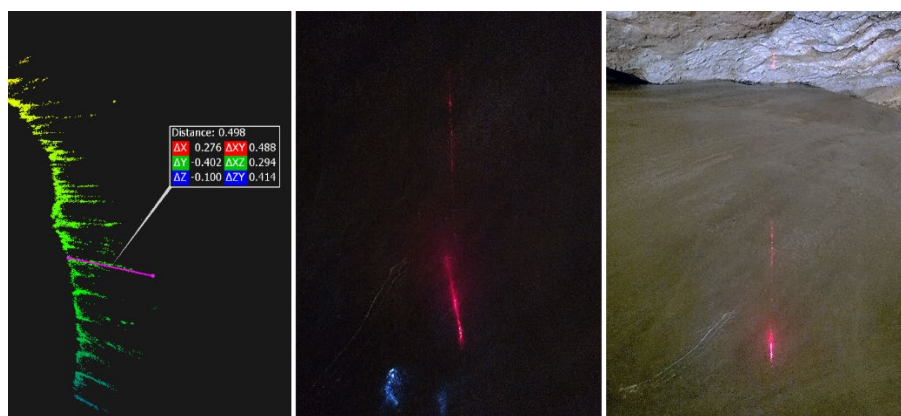


124 As a crystalline form of water, ice in a cave has a variable structure that depends both on the surface and ambient temperature  
125 and on the admixture of overlaying rock material. In Dobšiná Ice Cave, we can observe various structural forms of ice: large  
126 ice crystals in the ice mass, which have a coarse, granular texture, smooth clear ice, ice containing dust or impurities of  
127 overlaying rock, as well as various forms of frost on the walls (Fig. 5). It can be clearly stated that the ice surface is variable  
128 depending on the position of the ice mass relative to the surface (floor ice and wall ice) as well as the ambient temperature.



129  
130 **Figure 5** Various types of ice surfaces in the cave (source: authors).

131  
132 Electromagnetic radiation has the ability to penetrate transparent materials - such as water and ice. The choice of surveying  
133 methodology must be considered in this context (Warren, 2019). Since the optical properties of ice influence the interpretation  
134 of measured data, the choice of an appropriate methodology for geodetic and geophysical mapping of ground ice in the cave  
135 certainly does not have a clear answer.



136  
137 **Figure 6** Penetration of the laser beam into the ice structure.



138

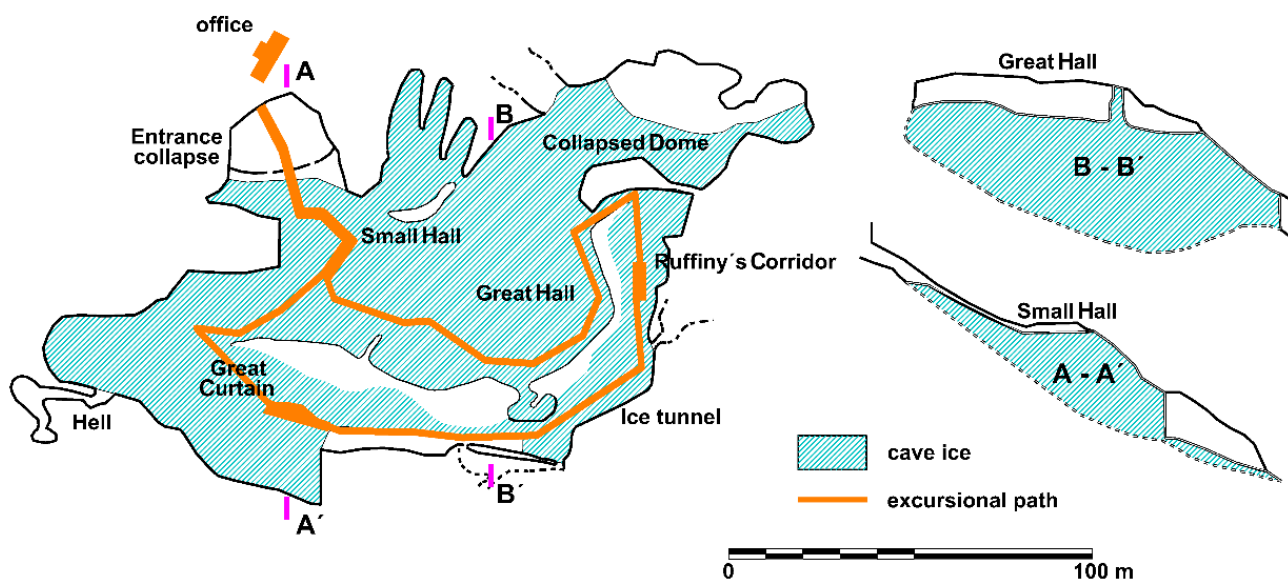
139 Figure 6 shows the penetration of the laser beam (TLS and digital tacheometry) through the ice structure, which can reach up  
140 to 0.5 m into the ice structure. Methods such as laser scanning and digital tacheometry are not suitable for very accurate  
141 measurements of ice surface topography, much less for detecting changes in ice-fill dynamics. Nevertheless, their use is in  
142 mapping the irregular shape of a cave's rock surface and other geodetic activities.

143

### 144 3.3 Establishment of the geodetic network

145

146 The geodetic survey started in 2011 on the initiative of the Slovak Caves Administration, and the measurements were carried  
147 out in several stages. The planimetric and altimetric measurements are carried out in the Slovak national coordinate system of  
148 the Uniform Trigonometric Cadastral Network (S-JTSK) and vertical datum Baltic Vertical Datum - After Adjustment (Bpv)  
149 from fixed points of the surveying net monumented in the ceiling parts of the cave. The basic prerequisite for the accurate  
150 evaluation of temporal and spatial changes in the ice fill of the cave (Fig. 7) is the existence of an underground geodetic control  
151 with the required density and accuracy.



152

153 **Figure 7** Cave floorplan and cross sections with ice filling in the cave (after Tulis et al., 1999).

154 The connection of the surface points of the Dobšinská Ice Cave network to the National Spatial Network was carried out  
155 through the Slovak Real-Time Positioning Service (SKPOS), using signals from Global Navigation Satellite Systems (GNSS)  
156 by a static method for a duration of 3 hours, whereby the points of the orientation line 5001-5002, approximately 1047 m apart,  
157 were determined. Underground points 5004 to 5012, monumented in the solid, unweathered parts of the cave rock ceiling by





158 surveyor's nails, as well as points monumented by retro-reflective targets, were determined in 2011 from the orientation line.  
159 Since 2018, the point field has been complemented in several stages (Fig. 9), taking advantage of the drilled mine  
160 monumentation with reflective targets, with new survey marks monumented in the side walls and cave ceiling.

161 The point monumentation and marking were realized by the following methods (Fig. 8):

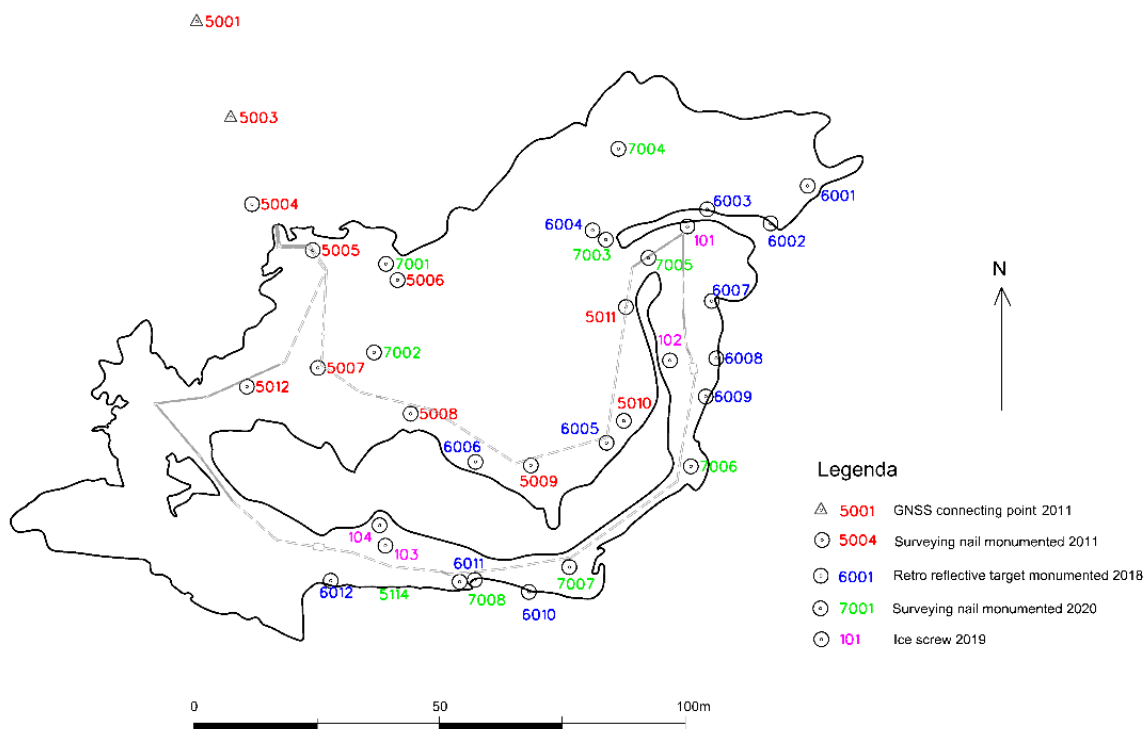
- 162 a) surveying nail in the cave ceilings,
- 163 b) drilled nail in the cave ceilings/wall,
- 164 c) surveying prism with reflective foil,
- 165 d) Leica retro-reflective target (2cm x 2cm) on an invar strip glued to the cave wall,
- 166 e) ice screw with leica retro-reflective target (2cm x 2cm),
- 167 f) ice screw with 12-bit coded target (2cm x 2cm x 3mm) for photogrammetry,
- 168 g) A4 paper 12-bit coded target for photogrammetry,
- 169 h) 12-bit coded target (2cm x 2cm x 3mm) glued to the cave wall for photogrammetry.



170  
171 **Figure 8** Monumentation of points of the geodetic point field and photogrammetric points and their marking.  
172

173 The geodetic network as a whole after the 2011 adjustment in the 2D cartographic plane can be characterized by a mean  
174 position error of 4.9 mm and a mean coordinate error of 3.5 mm. The mean error of the adjusted heights had a value of 1.7 mm  
175 for the height adjustment of the points. The standard error ellipses of the local geodetic network are represented by an estimate  
176 of the standard deviation of measured lengths of 1.4 mm and directions of 1.49 mgon for the Leica Viva TS15 motorized total  
177 station.





179

180 **Figure 9** Geodetic point field in the cave.

### 181 **3.4 Digital tacheometry**

182 In order to provide original knowledge about speleoclimatic and glaciological patterns in Dobšiná Ice Cave, their seasonal and  
183 trend changes, the first two stages of detailed spatial surveying of its upper part, formed by the Small and Great halls, were  
184 carried out. A detailed 3D model of the cave entrance and its underground spaces is being built on the basis of tacheometry,  
185 terrestrial laser scanning, and digital photogrammetry and in synergy with the existing climate monitoring system of the cave  
186 managed by the Slovak Caves Administration in Liptovský Mikuláš. In the future, it will serve as a basis for detailed scientific  
187 analyses of the state and development of the glaciation of the cave system in the environment of geographic information  
188 systems. The first measurements of the ice fill were made in 2011. However, regular and accurate measurements have been  
189 carried out from 2018 to the present. Detailed spatial measurements of the Small Hall and the Great Hall in the cave are carried  
190 out semi-annually using a motorized total station Leica Viva TS15 and a Trimble®VX™ Spatial Station in the months of May  
191 (before the start of the tourist season / after winter) and October (after the end of the tourist season / before winter). The  
192 positional and vertical connection was realized to the original and complemented survey points of the underground geodetic  
193 point field in the binding national coordinate system and vertical datum. Complete inter-annual and inter-semi-annual  
194 (seasonal) measurements of the change in floor ice height will be analyzed in a separate paper.

195



196 **3.5 Terrestrial laser scanning and SLAM technology**

197 The survey of the ice cave was realized by terrestrial laser scanning (TLS) in October 2018. More than 85 million points from  
198 30 survey stations were measured with a compact all-in-one full panoramic pulse laser scanner Leica ScanStation C10 (Fig.  
199 10 - left) and Leica HDS 6" targets with a laser beam in visible green EMR with wavelength 532 nm. The accuracy of a single  
200 measurement in position is 6 mm, in the distance 4 mm, and angle accuracy (horizontal/vertical) is 60  $\mu$ rad / 60  $\mu$ rad (12" /  
201 12"). The precision of modeled surface is 2 mm. The spatial resolution of 30  $\times$  30 mm of the final point cloud was achieved.  
202 Point clouds were processed in the computer-aided design software Leica Cyclone. We used a triangular mesh generation  
203 method by the Poisson Surface Reconstruction algorithm (Bolitho et al., 2007) to create the 3D MESH model, where surfaces  
204 are represented as a polygonal mesh.

205 In 2021, the Slovak Caves Administration (SCA) started monitoring the ice of the Dobšiná Ice Cave by monitoring its volume  
206 changes using a mobile 3D scanner Zeb Horizon from GeoSlam (Fig. 11 - right). The scanning is carried out on the trail of the  
207 guided tour and in its surroundings, with the circuit divided into two (approx. 20 min) scans. During the scanning of the first  
208 part, it is connected to 5 monumented survey points for georeferencing purposes (in post-processing), and to 6 points in the  
209 second part.



210  
211  
212 **Figure 10** Leica Scanstation C10 (left) and GeoSLAM measuring (right).

213  
214 Since the EMR penetrates the ice surface, the laser scanner survey was only used to model the overall shape of the cave itself,  
215 not to model changes in the ice surface accurately.



### 216 3.6 Digital close-range photogrammetry

217 Due to the specific characteristics and shapes of the ice surface, or their location and accessibility, some parts of the cave have  
218 been mapped and monitored semi-annually by digital close-range photogrammetry - the Structure-from-Motion (SfM) method,  
219 since 2018. These parts are as follows (see Fig. 11):

- 220 1. *vertical ice wall in Ruffiny's Corridor* (digital tacheometry and TLS are not possible due to the size of the vertical  
221 surface, large height differences, and limited space for movement),
- 222 2. *an artificial tunnel through the ice massif* (digital tacheometry and TLS are not possible due to the specific ice surface  
223 in the tunnel characterized by a significant penetration of the laser beam under the ice surface),
- 224 3. *a site in the part of the Great Curtain below the ice massif* at the interface between the ice and the bedrock (TLS is  
225 not possible due to the site and the limited space; however, total station measurements are used to track the position  
226 of the observation points accurately).



227  
228 **Figure 11** Localities of the photogrammetric survey.

229  
230 The Structure-from-Motion (SfM) photogrammetric method is used at all three sites. SfM is currently one of the most advanced  
231 photogrammetric processing techniques. It is originally based on computer vision and visual perception but has been gradually  
232 adapted to photogrammetry to derive three-dimensional structure from two-dimensional images of objects. The principle of





233 SfM is to estimate the 3D structure of a spatial object from two-dimensional image sequences originating from a moving  
234 recording medium. The advantage of SfM is the simultaneous image matching, bundle adjustment, and reconstruction of a 3D  
235 structure on images. The principle itself, the sequence of individual processing steps, and the corresponding algorithms are  
236 generally well-known and frequently used (Seitz et al., 2006; Westoby et al., 2012; Remondino et al., 2014; Pavelka et al.,  
237 2018; Štroner et al., 2020; and others).

238 From the principle of SfM and image matching, it follows that the success of this method strongly depends on the structure  
239 and texture of the imaged surface. In the case of:

- 240 ● flat and uniform texture,
- 241 ● surfaces with high reflectivity,
- 242 ● transparent surfaces,

243 the image matching may fail and result in too noisy data or no data at all. In ice caves, especially reflectivity and transparency  
244 of the ice surface can make the SfM unusable. This is also the case with the artificial tunnel in Dobšinská Ice Cave (Figs. 11  
245 and 15a-b). In order to be able to suppress reflections and refractions of light from the ice surface and thus use the SfM  
246 photogrammetry, we proposed to apply a cross-polarized photogrammetry (Wells et al., 2005; Edwards, 2011; Conen et al.,  
247 2018; Marčíš et al., 2018). This encompasses a polarized light source (stronger than other sources or the only source of  
248 illumination in the cave), in our case, a polarizing sheet attached directly to a DSLR camera flash, and a second polarizing  
249 filter attached to the DSLR camera lens. A prerequisite for cross-polarisation is that the polarizer on the lens must be rotated  
250 at 90° with respect to the polarizer on the flash.

251 We use a digital camera DSLR Pentax K-5 with the lens Pentax SMC DA 15 mm f/4 ED AL Limited for all three parts  
252 surveyed by photogrammetry. All images are taken using a tripod, 12-sec self-timer, ISO 200, aperture f/10 - f/13, and RAW  
253 format with subsequent conversion to 12-bit TIFF. Acquired images are processed in Agisoft Metashape® Professional  
254 Edition, Version 1.6.0 software (Agisoft LLC, St. Petersburg, Russia, 2019) by standard photogrammetric processing.

### 255 3.7 Geophysical methods

256 Methods of applied geophysics are based on precise measurements of physical fields, which are caused or influenced by  
257 structures with anomalous physical properties in the underground. These methods are used to detect and identify various  
258 subsurface objects – from shallow to larger depths (meter to kilometer scales). Application areas come from a large interval:  
259 from geological and tectonic studies and exploration of mineral deposits to very shallow applications in the detection of  
260 archaeological objects (near surface geophysics). Based on the kind of the studied physical field, applied geophysics is divided  
261 into various methods: gravity methods (gravimetry), magnetic methods (magnetometry), geoelectrical and electromagnetic  
262 methods, seismic and seismological methods, radiometric methods, etc. (Telford et al., 1990; Milsom and Eriksen, 2011;  
263 Reynolds, 2011). Determination of the thickness of ice layers represents a quite well-posed problem formulation for several  
264 methods in near-surface geophysics because there exists a quite large contrast in selected physical properties between the ice  
265 and its rocky basement (for instance, density, electrical permittivity, and conductivity, velocity of mechanical waves). Based

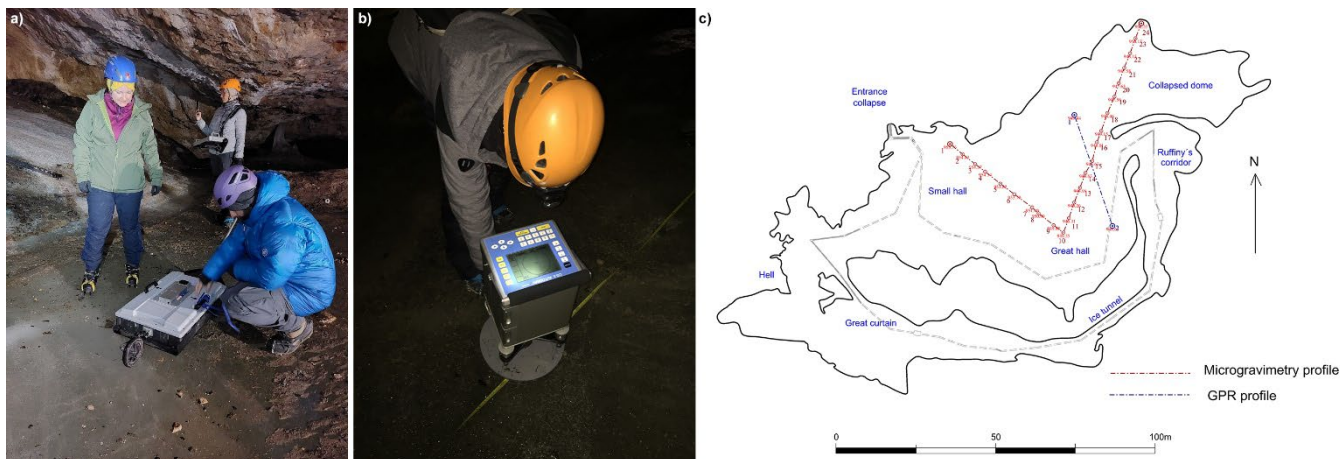


266 on the general knowledge from applied geophysics, a combination of several geophysical methods is often necessary – because  
267 various methods can support or debar outputs of them (each of the method is reacting to different physical properties of  
268 subsurface structures). From a great variety of near-surface geophysical methods, we have selected in this study the  
269 microgravity method (very precise gravimetry) and ground penetrating radar method (GPR), which is one of the most effective  
270 electromagnetic methods in near-surface geophysical applications.

### 271 3.7.1. Gravimetry

272 Gravimetry, or its specific detailed version - microgravimetry, is a geophysical method to measure and interpret very small  
273 changes in gravity acceleration. In microgravimetry, gravity changes (anomalies) that are caused by shallow subsurface objects  
274 with a significant density contrast to the surroundings are particularly interesting, for instance, crypts in archaeology (Pašteka  
275 et al., 2020), mines (Bishop et al., 1997) and caves (Butler, 1984). Due to its low density compared to the surrounding rocks,  
276 the ice filling of caves can also be a subject of interest for gravimetry. In the case of ice filling, we can basically talk about two  
277 possibilities for using gravimetry. The first method is mapping the thickness of the ice fill based on the complete Bouguer  
278 anomaly (CBA) calculation and subsequent density modeling. This methodology requires the necessary corrections for the  
279 topography, as well as corrections for the cave spaces themselves.

280 The second methodology is repeated monitoring of changes in gravity acceleration due to volume changes of the ice filling.  
281 For this purpose, test gravity measurements along the V-shaped profile were carried out at the site (Fig. 12 - right) in 2020 and  
282 2022. A Scintrex CG-5 gravity meter was used for the measurements. A stable base point (on rocky ground) was located inside  
283 the cave, on which measurements were taken to check the drift of the gravity meter. The reference point was located outside  
284 the cave. Measuring on ice is not easy, as the ice is easily deformed under the measuring tripod due to the weight of the  
285 gravimeter, which makes measurement very problematic. That is why we also used a special steel pad for the measurement,  
286 which better distributes the pressure on the surface of the ice (Fig. 12 - left). Stabilization of the steel pad on the sloping surface  
287 of the ice filling is also problematic. The estimated error of the gravity measurement from the control measurements is at the  
288 level of approx.  $5 \mu\text{Gal}$  ( $5 \cdot 10^{-8} \text{ m/s}^2$ ). Measured gravity changes between 2020-2022 reach one order higher values (up to  
289 approximately  $50 \mu\text{Gal}$ ), so we can discuss a reliable measurement.



290

291 **Figure 12** Example from GPR (a) and gravity (b) measurements along a selected line in the Dobšiná Ice Cave (c) (used  
292 instrument: MALA GroundExplorer GX with 160 MHz antenna (a) and Scintrex CG-5 gravity meter (b)).

293

### 294 3.8 Ground penetrating radar

295 As mentioned in the upper part of this contribution, electromagnetic emission (EM) can penetrate through lucent materials and  
296 environments – also through ice medium. In the case of the GPR method (familiarily georadar), electromagnetic emission is  
297 created by a transmitting antenna of the instrument to study the subsurface's structure (Fig. 12 - left). In the case of the GPR  
298 method, electromagnetic emission usually has frequencies that are outside the interval of visible light – these usually have a  
299 value of hundreds of MHz (typical values are from 100 to 500 MHz). Transmitted pulses of EM emission are reflected from  
300 subsurface objects, and after their return back to the surface, these are registered by a receiver antenna of the instrument.  
301 Registered reflections of EM emissions are then processed by means of special methods due to the wave character of the  
302 acquired data, and vertical time-sections (so-called radargrams) are usually the first outputs for geological or geotechnical  
303 interpretation (for instance, Milsom and Eriksen, 2011) (Fig. 17a). It is also important to mention that the recorded and  
304 displayed time in these sections is the so-called two-way-time (TWT) because this is the time, which the EM pulse has traveled  
305 from the emitting source to the reflecting object and then back to the registration in the instrument. In the process of  
306 recalculation of the TWT values, these must be then halved. Precise positions of the surface measurements are usually obtained  
307 through terrestrial geodetic methods and/or using GNSS technology. The local position of the instrument along measuring  
308 lines is determined by means of an odometer wheel.

309 During the processing and interpretation of acquired GPR data, a very important parameter is the velocity of EM radiation in  
310 the subsurface medium – this value is influenced by the electromagnetic physical properties of soils, rocks, and ice. There exist



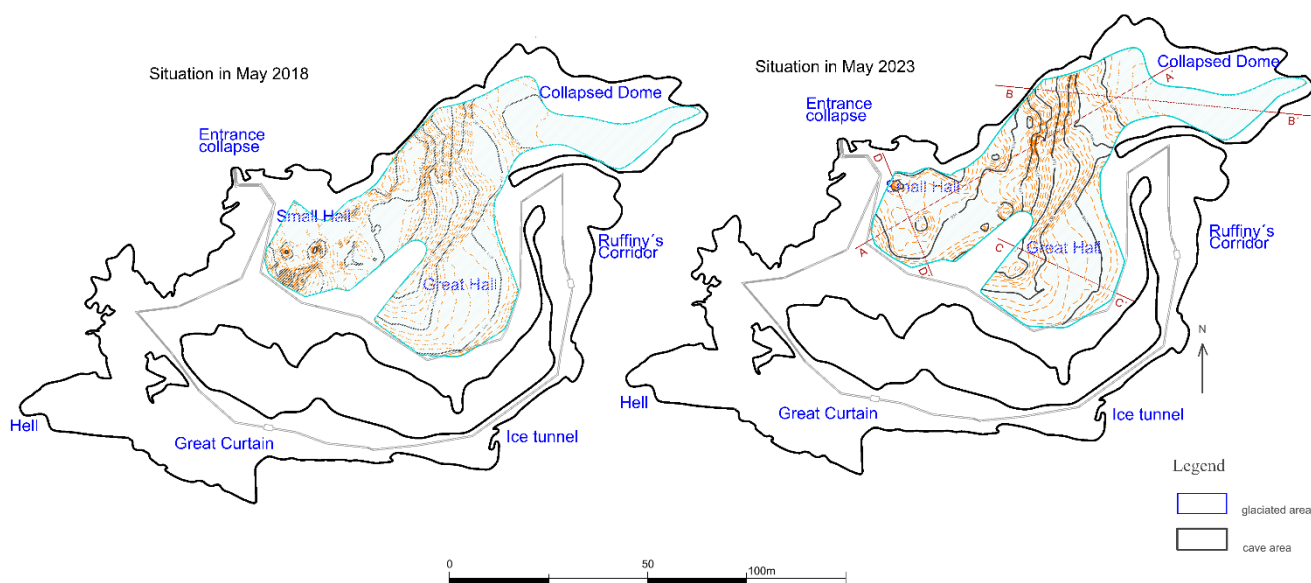


311 several methods for velocities estimation, and one of them is widely used: fitting the shape of a selected diffraction wave of  
312 hyperbolic shape in the vertical time section. Typical values of the velocities for various types of ice (from freshwater ice to  
313 permafrost environments) vary in quite large intervals from 0.15 to 0.3 m/ns (for instance, Reynolds, 2011). In the case of the  
314 ice in ice caves, it can be expected that these values will be closer to the lower limit of this interval. For example, we can  
315 mention typical values for the ice-sheet margin in East Antarctica, where the average value equals 0.18 m/ns (Guo et al., 2022).  
316 After using estimated velocity values to the TWT data, typical depths achieved by the GPR method are first meters; in the case  
317 of lower electrical permittivity, these can reach depths of 10 – 20 m (but this result depends strongly upon the used frequency  
318 of the GPR antenna). The GPR method was applied before with great success for the estimation of the thickness of ice in the  
319 case of continental or mountain glaciers (Singh et al., 2012; Navarro et al., 2018; Bello et al., 2020; Guo et al., 2022 and many  
320 others).

## 321 4 Results

### 322 4.1. Digital tacheometry

323 The ice fill is constantly changing its shape. Both external (precipitation, temperature) and internal factors (airflow velocity  
324 and direction, internal temperature, air pressure, humidity in the cave) influence the height of the floor ice in the cave during  
325 the year. The contour plots of both surfaces were made by processing the measured tacheometric data at two epochs in May  
326 2018 and May 2023 (Fig. 13).



327  
328 **Figure 13** Height and extent of glaciation in the Small Hall, Great Hall, and Collapsed Dome  
329

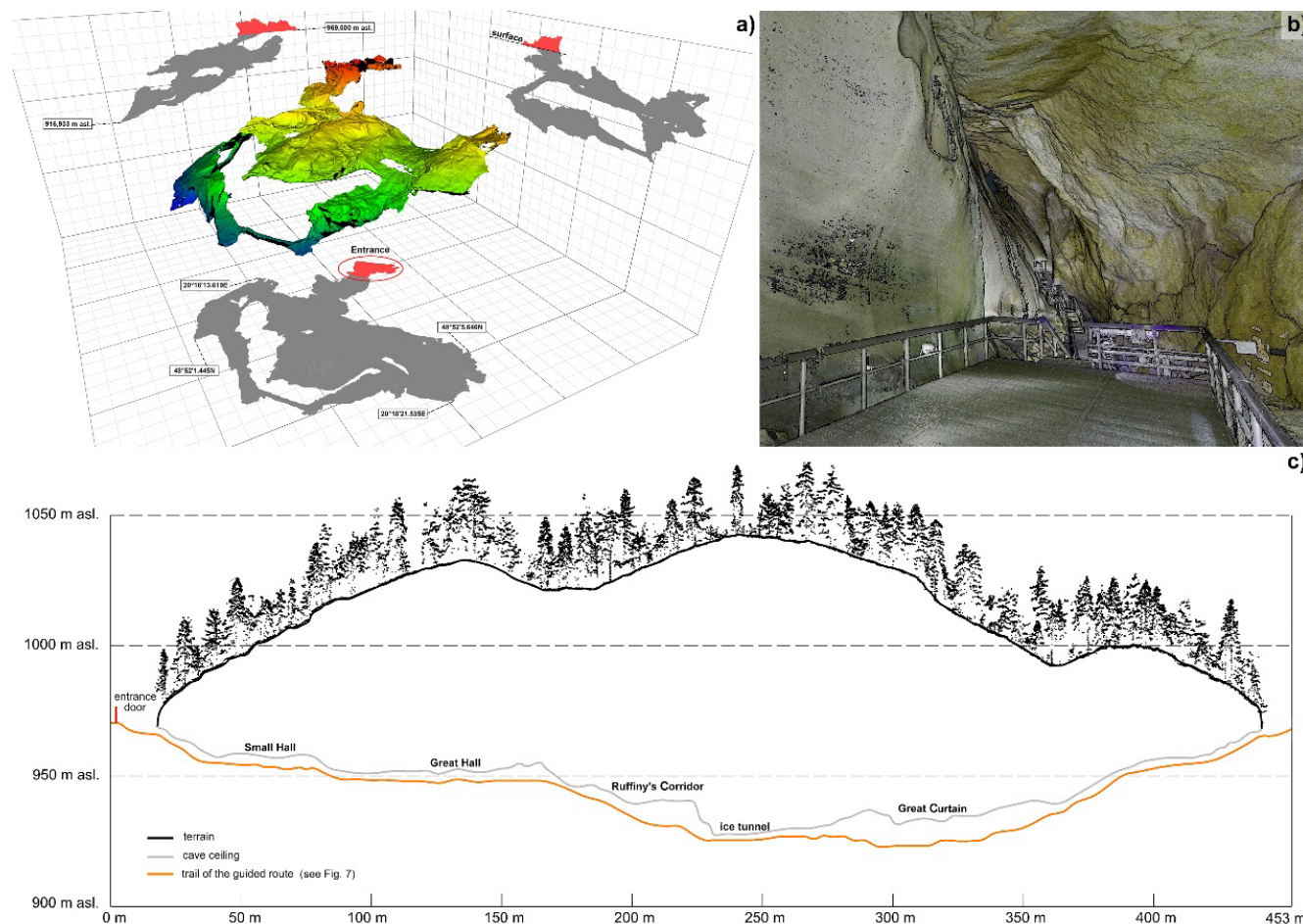


## 330 4.2. Terrestrial Laser Scanning and SLAM technology

331 TLS survey allows us to obtain a complete general point cloud and, thus, a 3D model of the glaciated part of the Dobšiná Ice  
332 Cave. Due to the penetration of the laser beam into the ice (Fig. 6), not all parts of the TLS point cloud are suitable for detailed  
333 analysis. However, these data can be used for visualization and presentation to show a general overview of the cave. Processing  
334 the point clouds from both terrestrial laser scanning and SLAM produced the resulting visualization shown in Figure 14a. The  
335 point cloud can also be viewed as freely available data on the web at  
336 [http://ugkagis.fberg.tuke.sk/potree/dobsinska\\_ladova\\_jaskyna/portal.html](http://ugkagis.fberg.tuke.sk/potree/dobsinska_ladova_jaskyna/portal.html).

337 A longitudinal cross-section through the trail of the guided tour in the cave and corresponding surface (classified point cloud  
338 from aerial laser scanning; ÚGKK SR) is shown in Fig. 14c.

339



340

341

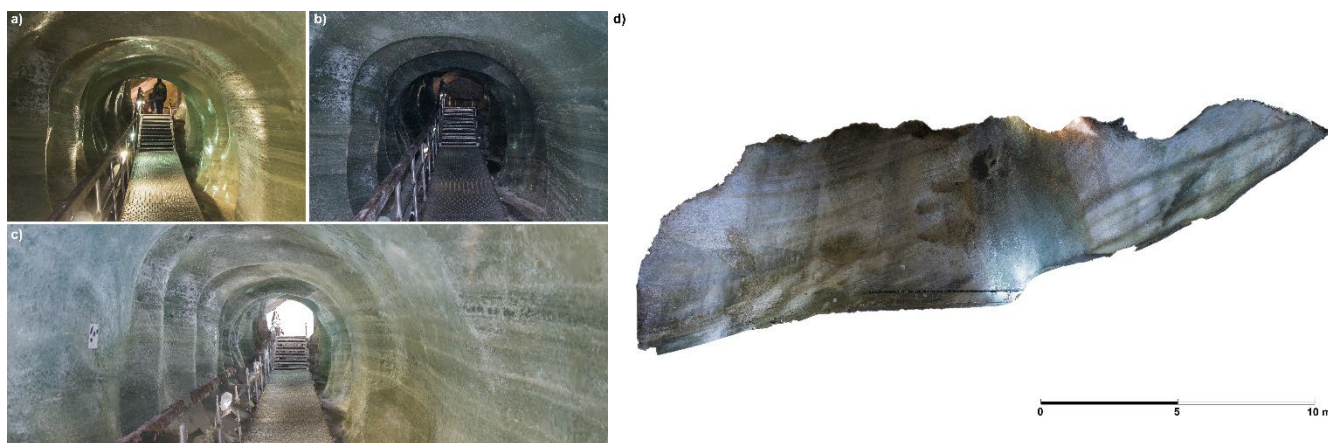
342 **Figure 14** a) a general overview of the final 3D MESH model; b) detail of the point cloud from laser scanning; c) a  
343 longitudinal cross-section through the cave (source of the terrain - LiDAR data: ÚGKK SR).



#### 344 4.3. Digital close-range photogrammetry

345 The results of digital photogrammetry confirmed the usability of the SfM method for 3D reconstruction of the ice filling  
346 surfaces in the selected parts of the cave with sufficient accuracy. By using cross-polarized photogrammetry, we are able to  
347 suppress light reflections from the ice successfully (Fig. 15). The main results of the SfM processing are dense point clouds,  
348 MESH models (Fig. 15), and for the Ruffiny's corridor also an orthophotomosaic.

349 The following Figure (Fig. 15) shows the effect of cross-polarization (DSLR camera with a mounted flash and polarizing filter  
350 on the lens and the flash rotated at 90° with respect to each other) on the reflections caused by artificial illumination on the ice  
351 surface (a-b). Figure 15c shows the final textured 3D MESH model generated by the SfM photogrammetry from cross-  
352 polarized images, and Figure 15d shows the final dense point cloud of Ruffiny's corridor. Both of them, the MESH model and  
353 dense point cloud, are compact, smooth, and without significant noise or holes. The only part with lower quality is the railing  
354 of the guided tour trail in the tunnel, but this railing is not necessary to determine the tunnel's spatial changes.



355  
356 **Figure 15** Results of the photogrammetric survey of the ice tunnel and Ruffiny's corridor; a) image without cross-polarisation,  
357 b) cross-polarized image; c) resulting 3D digital model of the tunnel; d) dense point cloud of the Ruffiny's corridor in 2018.

358 By comparing these results from individual epochs, we are able to determine changes in the ice filling over time. These results  
359 give us information about the direction and speed of the ice filling dynamics and also about changes in the volume of ice filling  
360 in these parts. Given the complexity of the issue and the amount of data, we provide a partial analysis of results for the 2018-  
361 2023 epochs only for the first two photogrammetric sites.

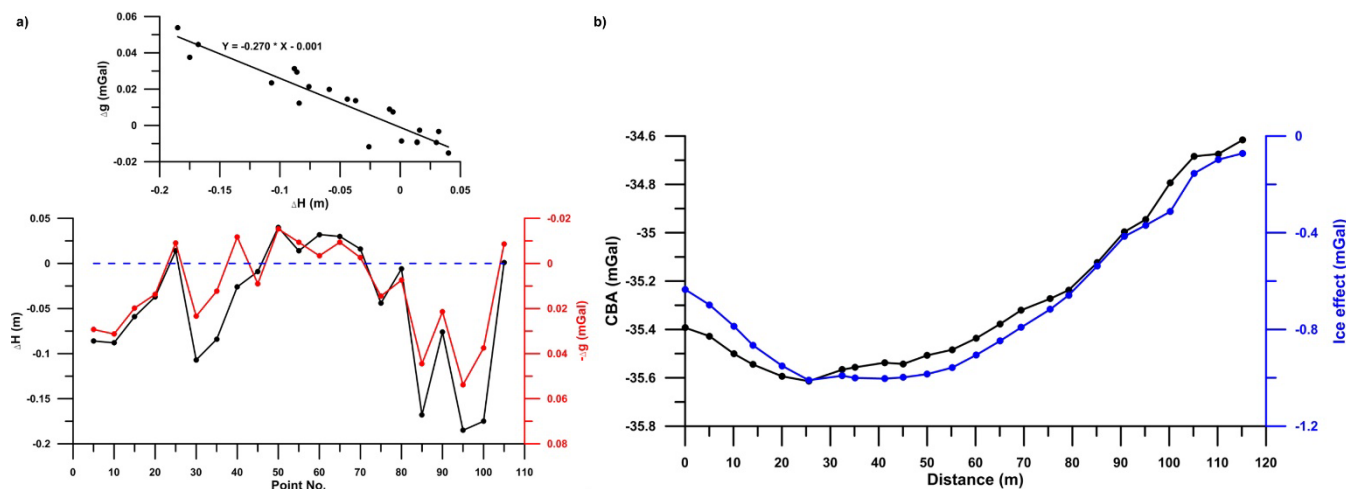
#### 362 4.4. Microgravimetry measurements in Dobšiná Ice Cave

363 The results of repeated test gravity measurements between the years 2020 - 2022 (Fig. 16) confirmed that given volume  
364 changes of the ice filling, which manifest themselves in height changes at the level of at least a few cm (or more), are reliably





365 detectable by gravimetric methods despite the difficult measurement conditions. Gravimetry can thus be used to monitor  
366 dynamic changes in the level of the ice fill.

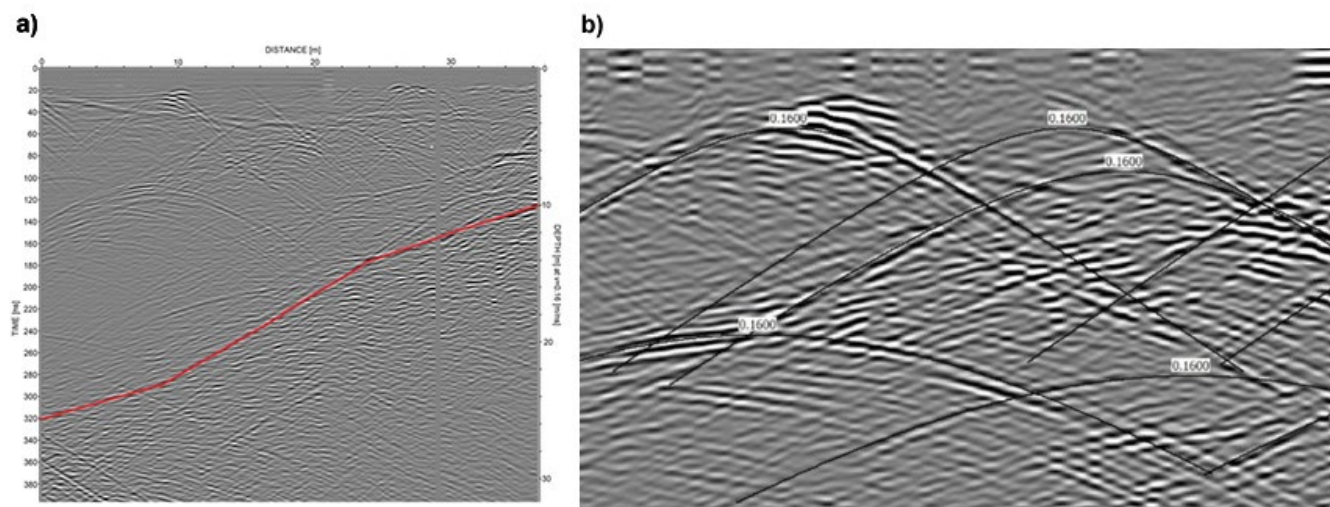


367

368 **Figure 16** (a) Grav-1: Correlation of measured height and gravity differences between the years 2020 - 2022 at test profile  
369 points. For a better comparison, the gravity differences (in red) are shown with the opposite sign. The blue dashed line shows  
370 zero differences. (b) Grav-2: Approximate comparison of the CBA (correction density 2670 kg/m<sup>3</sup>) and the gravitational effect  
371 of the ice fill (differential density -1750 kg/m<sup>3</sup>) along the test gravimetric profile.

#### 372 4.5. Ground penetrating radar

373 Tests of the GPR method during the years 2020-2022 in Dobšinská Ice Cave brought very interesting and promising results.  
374 Measurements have been performed by means of a MALA GroundExplorer GX instrument (with 160 MHz antenna) along the  
375 selected line in the cave. Basic processing steps have been performed with a focus on selecting the proper gain function (aiming  
376 to amplify reflection amplitudes from deeper positioned objects). As it can be seen in the processed vertical radargram from  
377 this site (Fig. 17a), the ice filling is characterized by a relatively homogeneous wave pattern – besides a relatively large amount  
378 of isolated diffraction waves (with the typical hyperbolic shape), coming with great probability from isolated stones and pieces  
379 of rocks in the ice. The average velocity, estimated from these diffraction waves (Fig. 17b), was set to 0.16 m/ns. In the selected  
380 vertical radargram (Fig. 17a), accepting the estimated velocity of 0.16 m/ns, the depth of the base of ice varies from 10 m to  
381 approx. 25 m below the ice surface (corresponding TWT values were 125 and 320 ns). The boundary between the ice and its  
382 basement is plotted with a thick red line in Fig. 17a.



383

384 **Figure 17** (a) Selected vertical radargram from the Dobšiná Ice Cave (left-hand vertical axis: two-way-time, right-hand axis:  
385 depth for the velocity 0.16 m/ns, the thick red line represents the boundary between the ice and the basement). (b) The selected  
386 part of a vertical radargram with plotted diffraction waves and estimated values of the EM wave velocity (0.16 in this case).

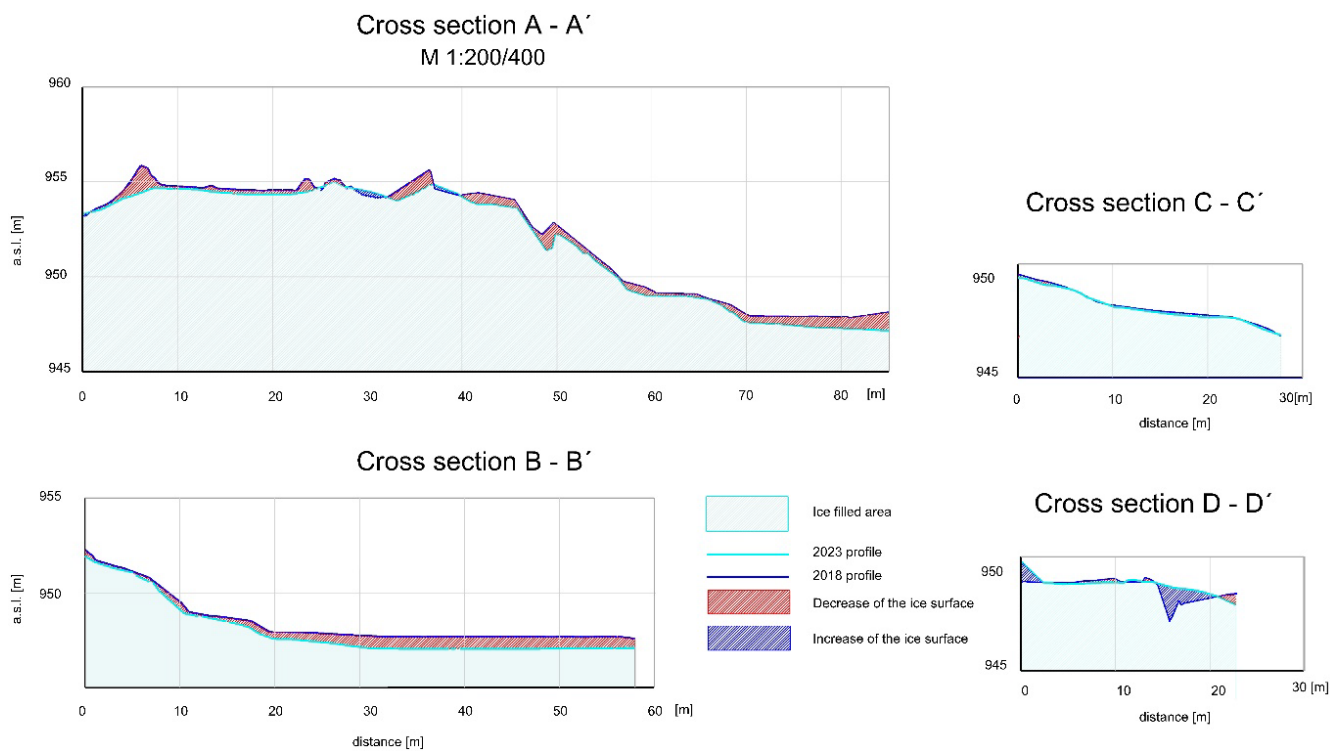
## 387 5 Discussion

388 Different surveys of the cryosphere, and especially of ice caves, have been part of their documentation for many years. There  
389 are measurements of ice extent, ice surface characteristics, the volume of ice filling in caves, spatio-temporal dynamics of the  
390 ice bodies, and others. Analyses of dynamics of the ice in caves have been presented in several papers (Strug and Zelinka,  
391 2008; Perşoiu and Pazdur, 2011; Gómez-Lende and Sánchez-Fernández, 2018; Perşoiu et al., 2021). Also, the ice measurement  
392 itself has been widely reviewed and presented (Gindraux et al., 2017; Alfredsen et al., 2018; Pfeiffer et al., 2022; Hruby, 2022).  
393 Authors Morard et al. (2010) recorded rapid changes in the Diablotins ice cave in Switzerland by monitoring the cave climate  
394 and suggested an hourly or daily monitoring interval based on a laser scanner or automatic cameras. The dynamics of ice  
395 bodies and their margins can also be monitored by data from a time-lapse camera and SfM photogrammetric processing  
396 (Mallalieu et al., 2017) or by UAS images and photogrammetric processing (Li et al., 2019). Over time, various technologies  
397 have been implemented and have been used with more or less success.

398 In this research, data from terrestrial laser scanning proved to be a good and quick technique to get a general spatial overview  
399 of the cave and the extent of the glaciated part with sufficient accuracy (Figs. 1, 10, and 14). However, determining changes  
400 in the ice volume by TLS can be problematic due to the properties of the laser beam incident on the ice surface. For this  
401 purpose, it is more appropriate to use digital tacheometry, which can provide a spatial position of individual points on the ice  
402 surface with high accuracy and, therefore, create a planimetric and altimetric map of the ice surface for individual epochs. The  
403 comparison of tacheometric data from years 2018 and 2023 revealed a significant loss of ice area, especially in the Small Hall

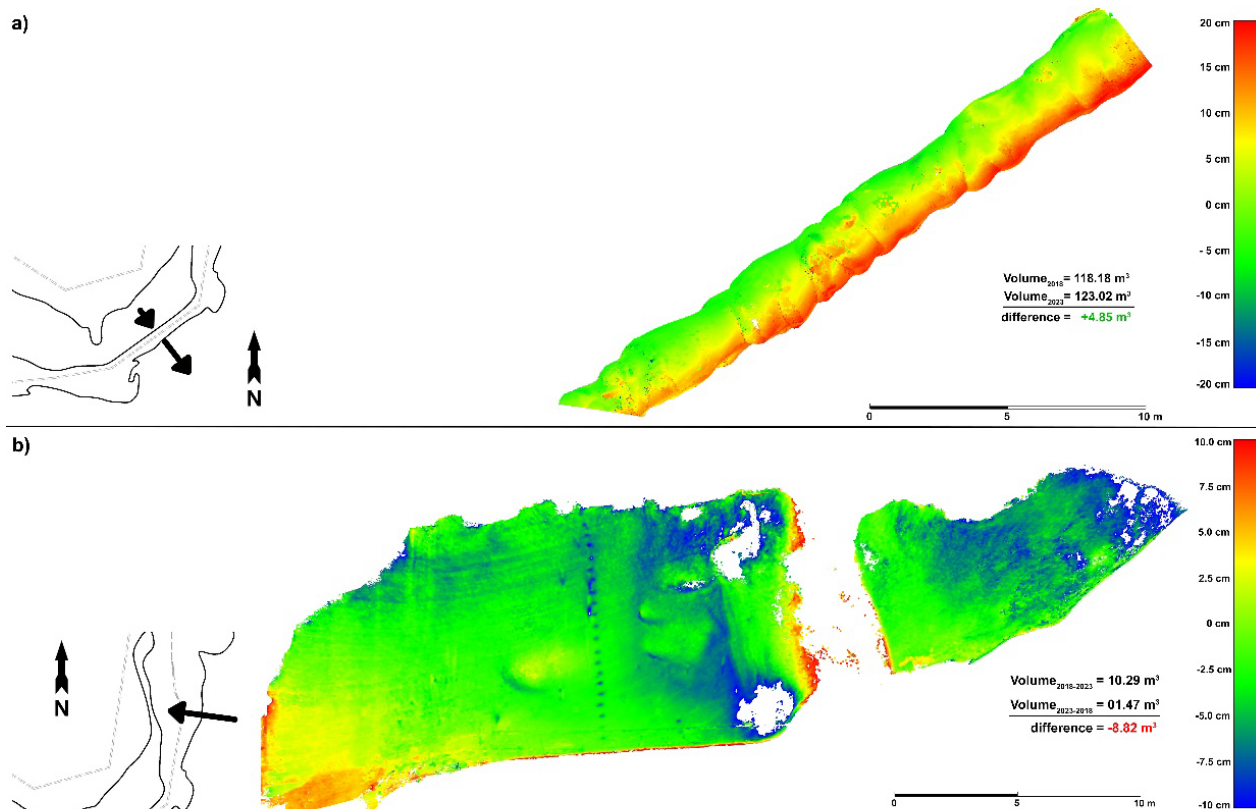


404 and Collapsed Dome parts (Fig. 18). The vertical loss of the ice level over the 5 years amounts to - 0.3 to - 0.9 m. By comparing  
405 the amount of glaciation over this five-year period, it can be clearly stated that the ice volume has increased by 99.5 m<sup>3</sup> in  
406 some places but decreased by up to 667 m<sup>3</sup> in others. In 2018, the area covered by ice was 2986 m<sup>2</sup>. Detailed inter-annual and  
407 inter-semi-annual (seasonal) measurements of the change in floor ice height will be analyzed in a separate paper.  
408



409  
410 **Figure 18** Longitudinal cross-sections through the Small Hall, Great Hall, and Collapsed Dome

411  
412 On the other hand, digital tacheometry is suitable for use only in parts with horizontal (floor) ice, where it is possible to measure  
413 the spatial position of points using a common surveying prism. For specific parts in terms of their geometry, spatial orientation,  
414 and texture/structure of the ice, digital close-range photogrammetry would be the best option. In Dobšíná Ice Cave, we  
415 identified several specific glaciated parts suitable for the photogrammetric measurements. Due to the extensiveness of the  
416 research, we present results for two of them.



417

418 **Figure 19** Results of the photogrammetric survey of the ice tunnel and Ruffiny's Corridor; a) image without cross-polarisation,  
419 b) cross-polarized image; c) resulting 3D digital model of the tunnel; d) top view on the difference model of the tunnel between  
420 epochs 2018-2023; e) front view on the difference model of the corridor between epochs 2018-2023.

421

422 Fig. 19a illustrates a difference model - i.e. spatial changes, for the ice tunnel between epochs 2018 and 2023. According to  
423 the difference model, we can say that the tunnel gradually but irregularly widens, with more significant changes in the southeast  
424 (S-E) direction. In the S-E wall, the ice surface has shifted by approx. 20 cm; while in the opposite N-W wall, the ice surface  
425 has shifted by only approx. 5-10 cm. The total volume of the tunnel has changed by +5 m<sup>3</sup>.

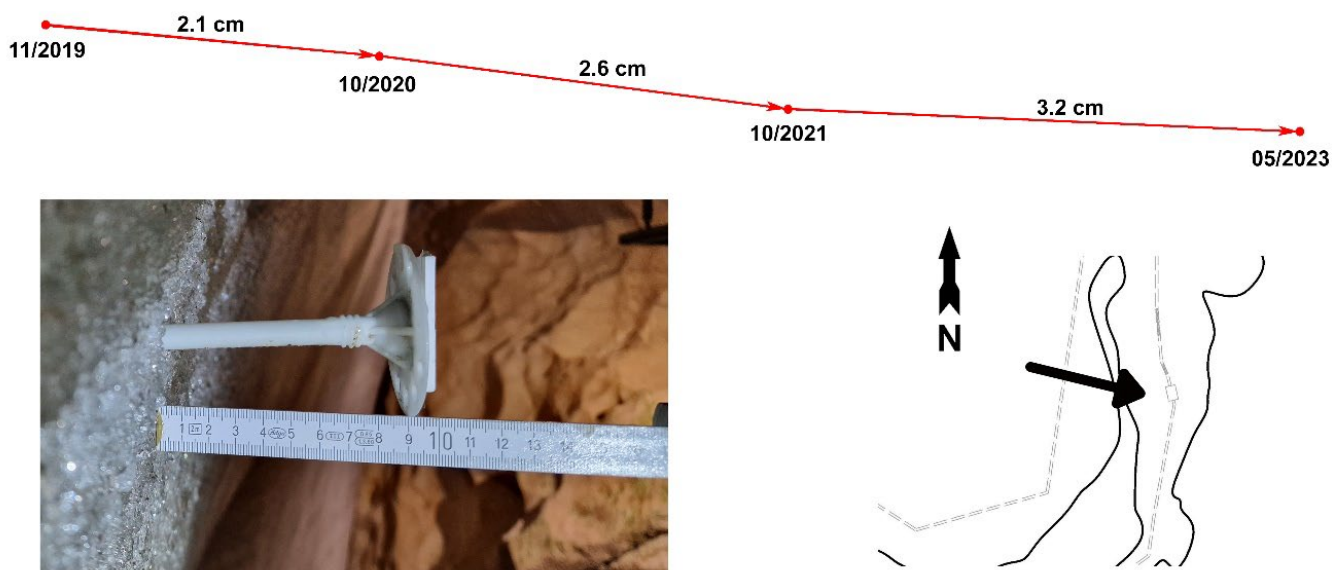
426 Fig. 19b illustrates a difference model for the vertical ice wall in Ruffiny's Corridor between epochs 2018 and 2023. According  
427 to the difference model, we can say that in some parts of the wall, the ice surface is slowly retreating (green to blue color), and  
428 in some parts, the ice surface is increasing (yellow to red), in the range of 0 - 10 cm. The blank parts of the difference model  
429 represent parts with changes larger than 10 cm. The highest increase is recorded in the icefall (vertical blank part, caused by





430 water slowly leaking from the upper parts) - more than 10 cm. The total change in the volume between 2018 and 2023 was  
431 recorded as an ice loss of  $-9 \text{ m}^3$ .

432 However, if we look at the geodetic point monumented as an ice screw into the vertical wall (Figs. 8 and 20) in 2019, there are  
433 two apparent movements. The first is the retreat of the ice surface by 9 cm (this displacement can also be partially caused by  
434 pushing the screw out of the ice by the ice solid itself, but there is no clear evidence of that). The second is a spatial displacement  
435 of the point by 2 cm (1-year period), 2,5 cm (1-year period), and 3 cm (1,5-year period). Therefore, there can be a combination  
436 of ice retreat, movement of the ice body, and extrusion of the screw from the ice. The spatial change of this point (and the ice  
437 wall) is almost in the same direction as in the case of the ice tunnel.



438  
439 **Figure 20** Spatial changes of the ice screw monumented in the vertical ice wall between 2019 - 2023.

440  
441 In terms of geophysical methods, both of them proved to be suitable and, what is more important, complementary to TLS,  
442 tacheometry, and photogrammetry since they can provide data which are not obtainable by geodetic methods (mainly the depth  
443 of the ice body and its structure under the surface).

444 This means, from the point of view of speleologists, it is also important to map the total volume of ice in the cave, which is,  
445 however, a methodologically more complex and demanding task. At this stage of the study of the Dobšiná Ice Cave, we are  
446 able, on the basis of the measurements so far, to at least tentatively assess the possibility of determining the total thickness of  
447 the ice filling based on the interpretation of the CBA. In the calculation of CBA, state-of-the-art procedures were used with



448 the use of Toposk software (Zahorec et al., 2017), detailed DEM5.0 based on aerial laser scanning  
449 (<https://www.geoportal.sk/sk/zbgis/lls-dmr/>, source: ÚGKK SR) and a spatial model of the cave derived from TLS and  
450 tachymetry. The calculated values of CBA along the profile were tentatively compared with the approximate calculation of  
451 the gravitational effect of the ice fill derived from the existing GPR measurements (Fig. 16b). A differential density of -1750  
452 kg/m<sup>3</sup> was used for the ice, as the difference between the actual density of approx. 920 kg/m<sup>3</sup> and the CBA correction density  
453 of 2670 kg/m<sup>3</sup>. The two curves are very similar, which indicates that gravimetry is potentially suitable for determining the total  
454 ice volume in the cave. This will require complex areal gravity mapping and subsequent 3D density modeling in the future.

455 In terms of ground penetrating radar, it has also been used in ice surveys for a long time. Dallimore and Davis (1992) used  
456 GPR to detect massive ground ice and map near-surface geology. GPR was also used in combination with SfM  
457 photogrammetry to describe the topography and ice thickness and determine the volume changes of a glacier in Greenland  
458 (Marcer et al., 2017). The usability of GPR technology to study permafrost rocks and the emergence of cryogenic processes  
459 was evaluated by Sokolov et al. (2020).

460 In Dobšiná Ice Cave, from repeated measurements along identical lines (acquired in both directions), the accuracy of the ice  
461 thickness could be estimated as the approximate value  $\pm 0.2$  m. This error is relatively high when compared with other geodetic  
462 methods, but the transition between ice and basement is not a clear boundary but a zone where the basement rocks are broken  
463 by the influence of ice. For this reason, a repetition of measurements along each line is so important. This kind of interpretation  
464 (estimation of ice thickness or the depth of ice basement) can be performed along a system of parallel and crossing lines, and  
465 an area map of these values can be plotted – contributing to a 3D model of ice cover in selected parts of the cave.

466 This research demonstrates that various geodetic (digital tacheometry, laser scanning, digital photogrammetry) and  
467 geophysical methods (microgravimetry, ground penetrating radar) are necessary for a comprehensive study of ice-filling  
468 dynamics in an ice cave, especially in terms of long-time monitoring. Ice bodies in caves can have different characteristics for  
469 individual parts of the cave, with changes in the structure and/or texture, even in a small area. Therefore, combining these  
470 methods can give us a comprehensive view of ice-fill dynamics and a suitable tool for long-term monitoring. However, we see  
471 a potential for using modern laser scanners that are available to filter reflected laser beams according to the number of the  
472 returned signal. Using such, it is possible to measure these surfaces in a comparable density and accuracy as with digital  
473 photogrammetry.

## 474 **6 Conclusions**

475 In this study, we review the current methodologies for surveying the ice filling and the thickness of the underground ice, and  
476 the dynamics of its evolution in the Dobšiná Ice Cave. We evaluated the suitability of using different geodetic and geophysical  
477 methods and technologies depending on the expected results. Due to the physical properties of the laser beam and its



478 penetration/reflection from the ice surface, as well as limiting factors in photogrammetric imaging, the use of different  
479 methodologies should be considered. We proposed the use of a tacheometric method to measure 3D data on the floor ice  
480 surfaces and a photogrammetric SfM method using cross-polarized light to measure the volumetric changes of ice in specific  
481 areas of the cave. We found the ground penetrating radar, geophysical method, and partial microgravimetry to be clearly  
482 successful in measuring the thickness of the ice. Modern ice cave research has not reached its zenith, and there is still room  
483 for improvement - depending on geodetic and geophysical measurement technology development. Since the underground  
484 glacier is characterized by its dynamic inter-annual changes, dependent on climatic developments in both the exterior and  
485 interior of the cave, as well as anthropogenic factors, there is a constant need for regular monitoring in order to preserve this  
486 unique natural phenomenon as much as possible. This research shows the high applicability and suitability of the combination  
487 of these methods and technologies to monitor spatio-temporal changes in ice caves over a long period.

#### 488 **7. Author contribution**

489 All authors contributed to the fieldwork. KP conducted the research, processed the laser scanning and tacheometry data, and  
490 wrote the manuscript. KB conducted the photogrammetric research, processed the photogrammetric data, and wrote the  
491 manuscript in the photogrammetric measurements section. JG conducted the geodetic point field research and monumentation  
492 with subsequent adjustments and processed the tacheometric measurements. RP performed the GPR measurements and wrote  
493 the GPR section of the paper, PZ and JP performed the gravimetry survey and wrote the gravimetry section, LK, EA and DB  
494 carried out all the necessary field measurements, PB led the work on the paper in terms of geomorphology and cave glaciations,  
495 as well as research guidance, LD carried out the SLAM measurements.

#### 496 **8. Competing interests**

497 The authors declare that they have no conflict of interest.

#### 498 **9. Acknowledgements**

499 We would like to thank everyone who contributed to the fieldwork, mostly Ľubomír Očkaik, the manager of the Dobšiná Ice  
500 Cave. Many thanks to the reviewers and the editor for their useful comments and suggestions.

#### 501 **10. Financial Support**

502 The study is the result of the Grant Project of the Ministry of Education of the Slovak Republic KEGA No. 003TUKE-4/2023  
503 and VEGA No.1/0340/22.

#### 504 **11. Data Availability Statement**

505 The raw data supporting the conclusions of this article will be made available by the authors, without undue reservation.



506 **References**

- 507 Alfredsen, K., Haas, C., Tuhtan, J. A. and Zinke, P.: Brief communication: Mapping river ice using drones and structure from  
508 Motion, *The Cryosphere*, 12(2), 627–633, doi:10.5194/tc-12-627-2018, 2018.
- 509 Behm, M.; Hausmann, H. Determination of ice thicknesses in alpine caves using georadar. In Proceedings of the 3rd  
510 International Workshop on Ice Caves, Kungur, Russia, 12–17 May 2008.
- 511 Bella, P.: Morphology of ice surface in the Dobšiná Ice Cave, in Proceedings of the 2nd international workshop on Ice caves,  
512 Demänová dolina, 2006, pp. 15–23.
- 513 Bella, P.: Ice surface morphology, *Ice Caves*, 69–96, doi:10.1016/b978-0-12-811739-2.00033-4, 2018.
- 514 Bella, P., Bosák, P., Pruner, P., Hercman, H., Pukanská, K., Bartoš, K., Gaál, L., Haviarová, D., Tomčík, P. and Kdýr, Š.:  
515 Speleogenesis in a lens of metamorphosed limestone and ankerite: Ochtiná Aragonite Cave, Slovakia, *International Journal of*  
516 *Speleology*, 51(1), 13–28, doi:10.5038/1827-806x.51.1.2397, 2021.
- 517 Bella, P., Braucher, R., Holec, J., Veselský, M., 2014. Datovanie pochovania alochtonných fluvialných sedimentov v hornej  
518 časti Dobšinskej ľadovej jaskyne (IV. vývojová úroveň systému Stratenskej jaskyne) pomocou kozmogénnych nuklidov  
519 [Cosmogenic nuclide dating of the burial of allochthonous fluvial sediments in the upper part of the Dobšinská Ice Cave (IVth  
520 evolution level of the Stratenská cave system), Slovakia]. *Slovenský kras*, 52, 2, 101–110 (in Slovak with English abstract).
- 521 Bella, P., Tulis, J., Zelinka, J., Papáč, V., Višňovská, Z., Haviarová, D., 2020. Dobšiná Ice Cave (Slovakia, Central Europe)  
522 and its unique underground glacier originated in the mid-mountain position of the moderate climate zone. *Aragonit*, 25(1), 4–  
523 16.
- 524 Bella, P., Zelinka, J.: Ice caves in Slovakia, *Ice Caves*, 657–689, doi:10.1016/b978-0-12-811739-2.00029-2, 2018.
- 525 Bello, C., Santillan, N., Cochachin, A., Arias, S., Suarez, W., 2020: Ice thickness using ground penetrating radar at Znosko  
526 glacier on King George island. Proceedings from 2020 IEEE Latin American GRSS & ISPRS Remote Sensing Conference,  
527 437-439
- 528 Berenguer-Sempere, F., Gómez-Lende, M., Serrano, E. and de Sanjosé-Blasco, J. J.: Orthothermographies and 3D modeling  
529 as potential tools in ice caves studies: The Peña Castil Ice Cave (Picos de Europa, Northern Spain), *International Journal of*  
530 *Speleology*, 43(1), 35–43, doi:10.5038/1827-806x.43.1.4, 2014.
- 531 Bolitho, M.; Kazhdan, M.; Burns, R.; Hoppe, H. Multilevel Streaming for Out-of-Core Surface Reconstruction. In Proceedings  
532 of the 5th Eurographics Symposium on Geometry Processing, Barcelona, Spain, 4–6 July 2007; pp. 69–78.
- 533 Bishop I., Styles P., Emsley S.J., Ferguson N.S., 1997: The detection of cavities using the microgravity technique: Case  
534 histories from mining and karstic environments. In: *Modern Geophysics in Engineering Geology*, 155-168. Geological Society  
535 Engineering Group, Special Publication No. 12, Geological Society, London.
- 536 Butler D.K., 1984: Microgravimetric and gravity gradient techniques for detection of subsurface cavities. *Geophysics* 49, 7,  
537 1084-1096.





- 538 Conen, N., Hastedt, H., Kahmen, O., Luhmann, T., 2018. Improving image matching by reducing surface reflections using  
539 polarising filter techniques. *The International Archives of the Photogrammetry, Remote Sensing and Spatial Information*  
540 *Sciences XLII-2*, 267–274. doi:10.5194/isprs-archives-xlii-2-267-2018
- 541 Dallimore, S.R. and Davis, J. (1992) Ground penetrating radar investigations of massive ground ice. In Pilon, J. A. (1992).  
542 *Geological Survey of Canada, Paper no. 90-4*, 241 pages, <https://doi.org/10.4095/133641>.
- 543 Edwards, N., 2011. Cross-polarisation, making it practical. *Journal of Visual Communication in Medicine* 34, 165–172.  
544 doi:10.3109/17453054.2011.635291
- 545 Faško, P., Šťastný, P., 2002. Mean annual precipitation totals. In *Landscape Atlas of the Slovak Republic*. Ministry of  
546 Environment of the Slovak Republic, Bratislava; Slovak Environmental Agency, Banská Bystrica (map No. 54, p. 99).
- 547 Gindraux, S., Boesch, R. and Farinotti, D.: Accuracy assessment of digital surface models from unmanned aerial vehicles'  
548 imagery on glaciers, *Remote Sensing*, 9(2), 186, doi:10.3390/rs9020186, 2017.
- 549 Gómez-Lende, M. and Sánchez-Fernández, M.: Cryomorphological topographies in the study of Ice Caves, *Geosciences*, 8(8),  
550 274, doi:10.3390/geosciences8080274, 2018.
- 551 Gómez-Lende, M.; Berenguer, F.; Serrano, E. Morphology, ice types and thermal regime in a high mountain ice cave. First  
552 studies applying terrestrial laser scanner in the Peña Castil ice cave (Picos de Europa, northern Spain). *Geogr. Fis. Din. Quat.*  
553 2014, 37, 141–150.
- 554 Guo J., Li, L., Liu, J., Fu, L., Tang, X., Wang, Y., Yang, W., Dou, Y., Liu, S., Lu, Q., Shi, G., Sun, Y., 2022: Ground-  
555 penetrating radar survey of subsurface features at the margin of ice sheet, East Antarctica. *Journal of Applied Geophysics* 206,  
556 104816
- 557 Hausmann, H. and Behm, M.: Imaging the structure of cave ice by ground-penetrating radar, *The Cryosphere*, 5(2), 329–340,  
558 doi:10.5194/tc-5-329-2011, 2011.
- 559 Hofierka J., Hochmuth Z., Kaňuk J., Gallay M., Gessert A.: Mapovanie jaskyne Domica pomocou terestrického laserového  
560 skenovania. *Geografický časopis* (2016) 68/1, s. 25-38.
- 561 Hruby, D.: For an otherworldly experience, venture into Europe's ice caves, 2022.
- 562 Kudla, M.: The history overview of the Dobšiná Ice Cave, *Aragonit*, 25(1), 17–23, 2020.
- 563 Korzystka, M., Piasecki, J., Sawiński, T. and Zelinka, J.: Climatic system of the Dobšinská Ice Cave, in 6th Congress of the  
564 International Show Caves Association , pp. 85–97, SNC of Slovak Republic, Slovak Caves Administration, Demänovská  
565 Valley, 2011.
- 566 Milius, J.; Petters, C. Eisriesenwelt—From Laser Scanning to Photo-Realistic 3D Model of the Biggest Ice Cave on Earth; GI-  
567 Forum: Washington, DC, USA, 2012; pp. 513–523.
- 568 Lalkovič, M.: Z histórie Dobšinskej ľadovej jaskyne, *Aragonit*, 5(1), 30–33, 2000.



- 569 Lapin, M., Faško, P., Melo, M., Šťastný, P., Tomain, J., 2002. Climatic regions. In Landscape Atlas of the Slovak Republic.  
570 Ministry of Environment of the Slovak Republic, Bratislava; Slovak Environmental Agency, Banská Bystrica (map No. 27, p.  
571 95).
- 572 Li, T., Zhang, B., Cheng, X., Westoby, M., Li, Z., Ma, C., Hui, F., Shokr, M., Liu, Y., Chen, Z., Zhai, M. and Li, X.: Resolving  
573 fine-scale surface features on Polar Sea Ice: A first assessment of UAS photogrammetry without ground control, Remote  
574 Sensing, 11(7), 784, doi:10.3390/rs11070784, 2019.
- 575 Mallalieu, J., Carrivick, J. L., Quincey, D. J., Smith, M. W. and James, W. H. M.: An integrated structure-from-motion and  
576 time-lapse technique for quantifying ice-margin dynamics, Journal of Glaciology, 63(242), 937–949, doi:10.1017/jog.2017.48,  
577 2017.
- 578 Marcer, M., Stentoft, P. A., Bjerre, E., Cimoli, E., Bjørk, A., Stenseng, L. and Machguth, H.: Three decades of volume change  
579 of a small greenlandic glacier using ground penetrating radar, structure from motion, and aerial photogrammetry, Arctic,  
580 Antarctic, and Alpine Research, 49(3), 411–425, doi:10.1657/aaar0016-049, 2017.
- 581 Marčíš, M., Barták, P., Valáška, D., Fraštia, M. and Trhan, O.: Use of image based modelling for documentation of intricately  
582 shaped objects, ISPRS - International Archives of the Photogrammetry, Remote Sensing and Spatial Information Sciences,  
583 XLI-B5, 327–334, doi:10.5194/isprsarchives-xli-b5-327-2016, 2016. Meyer, C.: History of ice caves research, in Ice Caves,  
584 Elsevier., 2018.
- 585 Milsom, J., Eriksen A., 2011: Field Geophysics. 4<sup>th</sup> edition, Wiley. ISBN 978-0-470-74984-5
- 586 Morard, S., Bochud, M. and Delaloye, R.: Rapid changes of the ice mass configuration in the dynamic diablottins ice cave –  
587 fribourg prealps, Switzerland, The Cryosphere, 4(4), 489–500, doi:10.5194/tc-4-489-2010, 2010.
- 588 Navarro, F.J., Martín-Español, A., Lapazaran, J.J., Grabiec, M., Otero, J., Vasilenko, E.V., Puczko, D., 2018: Ice Volume  
589 Estimates from Ground-Penetrating Radar Surveys, Wedel Jarlsberg Land Glaciers, Svalbard. Arctic, Antarctic, and Alpine  
590 Research 46, 2, 394-406
- 591 Novotný, L., 1993. Tret'ohorné jaskynné úrovne a zarovnané povrchy v Slovenskom raji [Tertiary cave levels and planation  
592 surfaces in the Slovak Paradise]. Slovenský kras, 31, 55–59. (in Slovak with English abstract)
- 593 Novotný, L., Tulis, J., 1996. Výsledky najnovších výskumov v Dobšinskej ľadovej jaskyni [Results of the newest researches  
594 in the Dobšiná Ice Cave]. Slovenský kras, 34, 139–147 (in Slovak).
- 595 Novotný, L., Tulis, J., 2005. Kras Slovenského raja [The karst of Slovak Paradise]. Správa slovenských jaskýň, Slovenská  
596 speleologická spoločnosť, Liptovský Mikuláš; Knižné centrum, Žilina, 175 p. (in Slovak with English summary).
- 597 Pavelka, K., Šedina, J. and Matoušková, E.: High resolution drone surveying of the Pista geoglyph in Palpa, Peru, Geosciences,  
598 8(12), 479, doi:10.3390/geosciences8120479, 2018.
- 599 Pašteka R., Pánisová J., Zahorec P., Papčo J., Mrlina J., Fraštia M., Vargemezis G., Kušnirák D., Zvara I., 2020: Microgravity  
600 method in archaeological prospection: methodical comments on selected case studies from crypt and tomb detection.  
601 Archaeological Prospection, 27, 415-431, https://doi.org/10.1002/arp.1787.



- 602 Petters, C.; Milius, J.; Buchroithner, M. Eisriesenwelt: Terrestrial laser scanning and 3D visualisation of the largest ice cave  
603 on earth. In Proceedings of the European LiDAR Mapping Forum, Salzburg, Austria, 29–30 November 2011.
- 604 Perşoiu A. and Lauritzen, S.-E.: in Ice caves, Elsevier, Amsterdam, Netherlands., 2018.
- 605 Perşoiu, A. and Pazdur, A.: Ice genesis and its long-term mass balance and dynamics in Scărișoara Ice Cave, Romania, The  
606 Cryosphere, 5(1), 45–53, doi:10.5194/tc-5-45-2011, 2011.
- 607 Perşoiu, A., Buzjak, N., Onaca, A., Pennos, C., Sotiriadis, Y., Ionita, M., Zachariadis, S., Styllas, M., Kosutnik, J., Hegyi, A.  
608 and Butorac, V.: Record summer rains in 2019 led to massive loss of surface and cave ice in SE Europe, The Cryosphere,  
609 15(5), 2383–2399, doi:10.5194/tc-15-2383-2021, 2021.
- 610 Pfeiffer, J., Rutzinger, M. and Spötl, C.: Terrestrial Laser scanning for 3D mapping of an alpine ice cave, The Photogrammetric  
611 Record, doi:10.1111/phor.12437, 2022.
- 612 Podshuhin, N.; Stepanov, Y. Measuring of the thickness of perennial ice in Kungur ice cave by georadar. In Proceedings of the  
613 3rd International Workshop on Ice Caves, Kungur, Russia, 12–17 May 2008, Kadebskaya, O., Mavlyudov, B.R., Pyatunin,  
614 M., Eds.; pp. 52–55.
- 615 Pukanská K., Bartoš, K., Bella P., Rákay S., and Sabová J.: Comparison of non-contact surveying technologies for modelling  
616 underground morphological structures, Acta Montanistica Slovaca, 22(3), 246–256, 2018.
- 617 Pukanská, K., Bartoš, K., Bella, P., Gašinec, J., Blistan, P. and Kovanič, L.: Surveying and high-resolution topography of the  
618 ochtiná aragonite cave based on TLS and digital photogrammetry, Applied Sciences, 10(13), 4633, doi:10.3390/app10134633,  
619 2020.
- 620 Ramspott, F.: Slovakia Country 3D Render Topographic Map Border. [online] Available from:  
621 <https://fineartamerica.com/featured/slovakia-country-3d-render-topographic-map-border-frank-ramspott.html> (Accessed 7  
622 July 2023), 2017.
- 623 Remondino, F., Spera, M.G., Nocerino, E., Menna, F., Nex, F., 2014. State of the art in high density image matching. The  
624 Photogrammetric Record 29, 144–166. doi:10.1111/phor.12063
- 625 Reynolds, J.M., 2011: An Introduction to Applied and Environmental Geophysics. 2<sup>nd</sup> edition, Wiley. ISBN 978-0-471-48535-  
626 3
- 627 Seitz, S.M., Curless, B., Diebel, J., Scharstein, D., Szeliski, R., n.d. A comparison and evaluation of Multi-View Stereo  
628 Reconstruction Algorithms. 2006 IEEE Computer Society Conference on Computer Vision and Pattern Recognition - Volume  
629 1 (CVPR'06). doi:10.1109/cvpr.2006.19
- 630 Singh, S.K., Rathore, B.P., Bahuguna, I.M., Ramnathan, A.L., 2012: Estimation of glacier ice thickness using Ground  
631 Penetrating Radar in the Himalayan region. Current Science 103, 1, 68-73



- 632 Smith K.J: Ice cave monitoring at Lava Beds National Monument. In: Land L., Kern Z., Maggi V. & Turri S. (Eds.),  
633 Proceedings of the Sixth International Workshop on Ice Caves. (2014), Idaho Falls, Idaho, USA: NCKRI Symposium 4.  
634 Carlsbad (NM): National Cave and Karst Research Institute, 88-93.
- 635 Sokolov, K., Fedorova, L. and Fedorov, M.: Prospecting and evaluation of underground massive ice by ground-penetrating  
636 radar, *Geosciences*, 10(7), 274, doi:10.3390/geosciences10070274, 2020.
- 637 Strug K. & Zelinka J. (2008) - The Demänovska Ice cave - The volume balance of the ice monolith in 2003-2007 (Slovakia).  
638 *Slovensky Kras*, 46, 369-386.
- 639 Štroner, M., Urban, R., Reindl, T., Seidl, J. and Brouček, J.: Evaluation of the georeferencing accuracy of a photogrammetric  
640 model using a quadrocopter with onboard GNSS RTK, *Sensors*, 20(8), 2318, doi:10.3390/s20082318, 2020.
- 641 Šťastný, P., Nieplová, E., Melo, M., 2002. Mean annual air temperature. Mean January air temperature. Mean July air  
642 temperature. In *Landscape Atlas of the Slovak Republic*. Ministry of Environment of the Slovak Republic, Bratislava; Slovak  
643 Environmental Agency, Banská Bystrica (maps No. 49–51, p. 98–99).
- 644 Šupinský, J., Kaňuk, J., Hochmuth, Z. and Gallay, M.: Detecting dynamics of cave floor ice with selective cloud-to-cloud  
645 approach, *The Cryosphere*, 13(11), 2835–2851, doi:10.5194/tc-13-2835-2019, 2019.
- 646 Telford, W.M., Geldart, L.P., Sheriff, R.E., 1990: *Applied Geophysics*. Cambridge University Press. ISBN 0-521-32693-1
- 647 Tulis, J., Novotný, L., 1989. Jaskynný systém Stratenskej jaskyne [The cave system of Stratenská jaskyňa Cave]. *Osveta*,  
648 *Martin*, 464 p. (in Slovak with Russian and English summary).
- 649 Tulis, J., Novotný, L., Bella, P., 1999. Dobšiná Ice Cave – nomination for inscription on the World Heritage List.  
650 Manuscript, ECS Slovakia Ltd., Spišská Nová Ves – Slovak Caves Administration, Liptovský Mikuláš – Ministry of the  
651 Environment of the Slovak Republic, 41 p.
- 652 Warren, S. G.: Optical properties of ice and snow, *Philosophical Transactions of the Royal Society A: Mathematical,*  
653 *Physical and Engineering Sciences*, 377(2146), 20180161, doi:10.1098/rsta.2018.0161, 2019.
- 654 Westoby, M.J., Brasington, J., Glasser, N.F., Hambrey, M.J., Reynolds, J.M., 2012. 'structure-from-motion' photogrammetry:  
655 A low-cost, effective tool for Geoscience Applications. *Geomorphology* 179, 300–314. doi:10.1016/j.geomorph.2012.08.021
- 656 Wells, J., Jones, T., Danehy, P., 2005. Polarization and color filtering applied to enhance photogrammetric measurements of  
657 reflective surfaces. 46th AIAA/ASME/ASCE/AHS/ASC Structures, Structural Dynamics and Materials Conference.  
658 doi:10.2514/6.2005-1887
- 659 Zahorec, P., Marušiak, I., Mikuška, J., Pašteka, R., Papčo, J., 2017: Numerical Calculation of Terrain Correction Within the  
660 Bouguer Anomaly Evaluation (Program Toposk), chapter 5, 79–92. In book: Pašteka, R., Mikuška, J., Meurers, B. (eds.):  
661 *Understanding the Bouguer Anomaly: A Gravimetry Puzzle*, Elsevier, ISBN 978-0-12-812913-5, doi 10.1016/B978-0-12-  
662 812913-5.00006-3